Electronic Supplementary Material (ESI) for ChemComm.

Supporting Information

$In[Ba_3Cl_3F_6]$: A Novel Infrared-Transparent Molecular Sieve Constructed by Halides

Xiaoqing Jiang,[a] Hongping Wu,[a] Hongwei Yu,[a,*] Zhanggui Hu,[a] jiyang wang,[a] Yicheng Wu[a]

[a]Tianjin Key Laboratory of Functional Crystal Materials, Institute of Functional Crystals, Tianjin University of Technology, Tianjin 300384, China.

CONTENTS

Section S1 Synthesis and characterization

1. Synthesis of $In[Ba_3Cl_3F_6]$ crystal.

$BaCl_2·2H_2O$ (99.5%), In_2O_3 (99.99%), and H_5IO_6 (99%) were obtained analytically pure from TianJin Fuchen, aladdin and aladdin respectively and used without any further purification. $In[Ba_3Cl_3F_6]$ was prepared by the mild hydrothermal method using $BaCl_2·2H_2O$ (1.6 g, 8 mmol), In_2O_3 (0.2 g, 1 mmol), H_5IO_6 (0.2 g, 1 mmol), 1ml HF (48%) and 3 mL deionized water. The mixture was stirred at room temperature for 30 minutes. Then it was sealed into a 30 mL teflon autoclave, heated to 220 °C in 3 hours and kept this temperature for 3 days. It was further slowly cooled to ambient temperature at a rate of 3 °C/h. Some high quality crystals were obtained and washed with deionized water and dried in air for single crystal structure determination. The X-ray powder diffraction patterns for $In[Ba_3Cl_3F_6]$ are shown in Figure S1.

2. Synthesis of $In[Ba_3Cl_3F_6]$ powder.

The method of synthesizing $In[Ba_3Cl_3F_6]$ powder is solid phase synthesis. The raw materials are BaF_2 (99%) and $InCl_3·4H_2O$ (99.9%) from aladdin. BaF_2 (3.21 g, 3 mmol) and $InCl_3·4H_2O$ (1.790 g, 1 mmol) were mixed and ground completed. Then the mixture was put in the muffle. The experimental process is heated to 300 °C in 50 minutes mantain the temperature for 5 h, and then slow cooled to ambient temperature. In this way, we can obtain the powder. The X-ray powder diffraction pattern for

$In[Ba_3Cl_3F_6]$ powder is shown in Figure S1.

3. Instruments and Methods.

Powder X-ray Diffraction.

The powder X-ray diffraction (XRD) data are collected using a PIGAKV Smart Lab 9KW with monochromatic Mo Kα radiation (λ= 1.5418 Å) at room temperature. The 2θ range is from 5 to 50° with a scan step width of 0.01° and a fixed counting time of 1.5 s per step. The powder XRD patterns of compounds are shown in Figure S1. Clearly, they are in agreement with the calculated pattern.

Energy-dispersive X-ray spectroscope.

Micro probe elemental analyses and the elemental distribution maps were measured on a field-emission scanning electron microscope (FESEM, Quanta FEG 250) made by FEI (Figures S2 and S3).

Thermal Analysis.

The thermal behavior of $In[Ba_3Cl_3F_6]$ was investigated by a simultaneous NETZSCH STA thermal analyzer instrument under the flow of N_2. The sample was enclosed in Al_2O_3 crucible and heated from 35 °C to 1300 °C at a rate of 10 °C /min.

Optical Measurement.

The IR spectrum was measured on Nicolet™ Continuμm™ IR Microscope and Nicolet iS50 FTIR Spectrometer made by Thermo-Fisher Business. The sample was put on the sample stage, and the spectrum was

collected in the range of 4000-400 cm^{-1}. The UV−VIS−NIR diffuse reflectance data for the monocrystal powder of In[$Ba_3Cl_3F_6$] was collected at room temperature using a UH4150 UV/VIS/NIR spectrophotometer with the measurement range extending from 300 to 2500 nm. Reflectance spectrum was converted to absorbance using the function $F(R)=\alpha/s=(1-R)^2/2R$ (α is absorbance, s is reflection coefficient), where R is the reflectance and F(R) is the Kubelka−Munk remission function.[1] The straightforward extrapolation method was used to deduce the band gap.[2] X-axis is $E=h\nu=hc/\lambda$ (hc=1240), (h is Planck constant, ν is Gamma frequency). Y-axis is F(R).

Textural properties of In[$Ba_3Cl_3F_6$].

The specific surface area and pore size distribution of the samples were measured by the physical adsorption apparatus of Autosorb-IQ3+chem Star made by Quanta-chrome in America. The data was collected in the N_2 atmosphere. The quality of the sample is 0.0596 g. The bath temperature is 77.35 K.

Single Crystal Structure Determination.

Single-crystal X-ray diffraction data for the compound was collected on the XtaLab Pro MM003Cu/Mo made by RIGAKU with Mo Kα radiation (λ=0.71073 Å) at 277 K. Data reduction was performed with CrysAlisPro, and absorption correction based on the multi-scan method was applied.[3] It was determined by the direct method refined by full-matrix least-squares

fitting on F^2 using SHELXL-97.[4] All of the non-hydrogen atoms were refined with anisotropic thermal parameters.[5] Crystallographic data and structural refinement of the compound are listed in Table S1, the atomic coordinates and equivalent isotropic displacement parameters for $In[Ba_3Cl_3F_6]$ are listed in Table S2. the selected bond distances and angles (deg) for $In[Ba_3Cl_3F_6]$ are listed in Table S3.

Table 1. Crystal data and structure refinement for $In[Ba_3Cl_3F_6]$.

Empirical formula	$In[Ba_3Cl_3F_6]$
Temperature	293(2) K
Wavelength	0.71073 nm
Crystal system	Trigonal
Space group	$P6_3/m$
Unit cell dimensions	a=10.1310(4) Å
	c=5.9315(3) Å
Z, Volume	2, 527.23(4) $Å^3$
Formula weight	149.44
Calculated density	2.353 mg/m^3
Absorption coefficient	7.003 mm^{-1}
F(000)	322
Crystal size	0.2974× 0.101 ×0.03996 mm^3
Theta range for data collection	4.02 to 29.65
Limiting indices	$-11\leq h \leq 13$, $-12 \leq k \leq 12$, $-7 \leq l \leq 8$
Reflections collected / unique	210 / 209
	[R(int)=0.030]
Completeness to theta=27.69	99.5%
Data / restraints / parameters	517 / 0 / 25
Goodness-of-fit on F^2	1.249
Final R indices $[F_o^2>2\sigma(F_o^2)]$[a]	R_1=0.0194
	wR_2=0.0413
R indices (all data)[a]	R_1=0.0212
	wR_2=0.0419
Extinction coefficient	0.0604(17)
Largest diff. peak and hole	1.21 and -1.27 $e\cdot Å^{-3}$

[a]$R_1 = \Sigma||F_o| - |F_c||/\Sigma|F_o|$ and $wR_2 = [\Sigma w(F_o^2 - F_c^2)^2 / \Sigma w F_o^4]^{1/2}$ for $F_o^2 > 2\sigma(F_o^2)$

Table S2. Atomic coordinates ($\times 10^4$) and equivalent isotropic displacement parameters ($Å^2 \times 10^3$) for $In[Ba_3Cl_3F_6]$. U_{eq} is defined as one-third of the trace of the orthogonalized U_{ij} tensor.

Atom	x	y	z	U_{eq}	BVS
Ba(1)	7017(1)	6138(1)	2500	10(1)	2.137
In(1)	3333	6667	2500	9(1)	3.064
Cl(1)	10612(1)	7906(1)	2500	19(1)	1.095
F(1)	3685(2)	8374(2)	190(3)	15(1)	0.94

Table S3. Selected bond distances (Å) and angles (deg) for $In[Ba_3Cl_3F_6]$.

Ba(1)-F(1)#1	2.7233(18)	F(1)#1-Ba(1)-F(1)#2	71.74(7)
Ba(1)-F(1)#2	2.7233(18)	F(1)#1-Ba(1)-F(1)#3	66.58(6)
Ba(1)-F(2)#3	2.8100(19)	F(1)#2-Ba(1)-F(1)#3	100.02(4)
Ba(1)-F(2)#4	2.8100(19)	F(1)#1-Ba(1)-F(1)#4	100.02(4)
Ba(1)-F(3)#5	2.9342(18)	F(1)#2-Ba(1)-F(1)#4	66.58(6)
Ba(1)-F(3)#6	2.9342(18)	F(1)#3-Ba(1)-F(1)#4	58.36(7)
Ba(1)-Cl(1)#7	3.1500(5)	F(1)#1-Ba(1)-F(1)#5	95.98(7)
Ba(1)-Cl(1)#8	3.1500(5)	F(1)#2-Ba(1)-F(1)#5	57.78(7)
Ba(1)-Cl(2)	3.1544(11)	F(1)#3-Ba(1)-F(1)#5	156.24(6)
Ba(1)-Cl(3)#9	3.1610(12)	F(1)#4-Ba(1)-F(1)#5	112.637(5)
Ba(1)-In(1)#10	3.9986(2)	F(1)#1-Ba(1)-F(1)#6	57.78(7)
Ba(1)-In(1)#11	3.9986(2)	F(1)#2-Ba(1)-F(1)#6	95.98(7)
In(1)-F(1)#12	2.0926(18)	F(1)#3-Ba(1)-F(1)#6	112.637(5)
In(1)-F(1)#13	2.0926(18)	F(1)#4-Ba(1)-F(1)#6	156.24(6)
In(1)-F(1)	2.0926(18)	F(1)#5-Ba(1)-F(1)#6	65.89(7)
In(1)-F(1)#14	2.0926(18)	F(1)#1-Ba(1)-Cl(3)#7	145.48(4)
In(1)-F(1)#4	2.0926(18)	F(1)#2-Ba(1)-Cl(3)#7	73.77(4)
In(1)-F(1)#3	2.0926(18)	F(1)#3-Ba(1)-Cl(3)#7	121.90(4)
In(1)-Ba(1)#15	3.9986(2)	F(1)#4-Ba(1)-Cl(3)#7	67.07(4)
In(1)-Ba(1)#7	3.9986(2)	F(1)#5-Ba(1)-Cl(3)#7	63.61(4)
In(1)-Ba(1)#16	3.9986(2)	F(1)#6-Ba(1)-Cl(3)#7	125.42(4)
In(1)-Ba(1)#8	3.9986(2)	F(1)#1-Ba(1)-Cl(3)#8	73.77(4)
In(1)-Ba(1)#10	3.9986(2)	F(1)#2-Ba(1)-Cl(3)#8	145.48(4)
In(1)-Ba(1)#11	3.9986(2)	F(1)#3-Ba(1)-Cl(3)#8	67.07(4)
Cl(1)-Ba(1)#1	3.1500(4)	F(1)#4-Ba(1)-Cl(3)#8	121.90(4)
Cl(1)-Ba(1)#17	3.1500(4)	F(1)#5-Ba(1)-Cl(3)#8	125.42(4)
Cl(3)-Ba(1)#18	3.1610(12)	F(1)#6-Ba(1)-Cl(3)#8	63.61(4)
F(1)-Ba(1)#8	2.7233(17)	Cl(3)#7-Ba(1)-Cl(3)#8	140.61(4)

F(2)-Ba(1)#13	2.8100(19)	F(1)#1-Ba(1)-Cl(3)	122.95(4)
F(3)-Ba(1)#15	2.9342(18)	F(1)#2-Ba(1)-Cl(3)	122.95(4)

Symmetry transformations used to generate equivalent atoms:

#1 x-y+1,x,-z #2 x-y+1,x,z+1/2 #3 -x+y,-x+1,z #4 -x+y,-x+1,-z+1/2

#5 y,-x+y,z+1/2 #6 y,-x+y,-z #7 y,-x+y+1,-z+1 #8 y,-x+y+1,-z

#9 -x+y+1,-x+2,z #10 -x+1,-y+1,-z #11 -x+1,-y+1,-z+1 #12 x,y,-z+1/2

#13 -y+1,x-y+1,z #14 -y+1,x-y+1,-z+1/2 #15 x-y,x,-z #16 x-y,x,-z+1

#17 x-y+1,x,-z+1 #18 -y+2,x-y+1,z

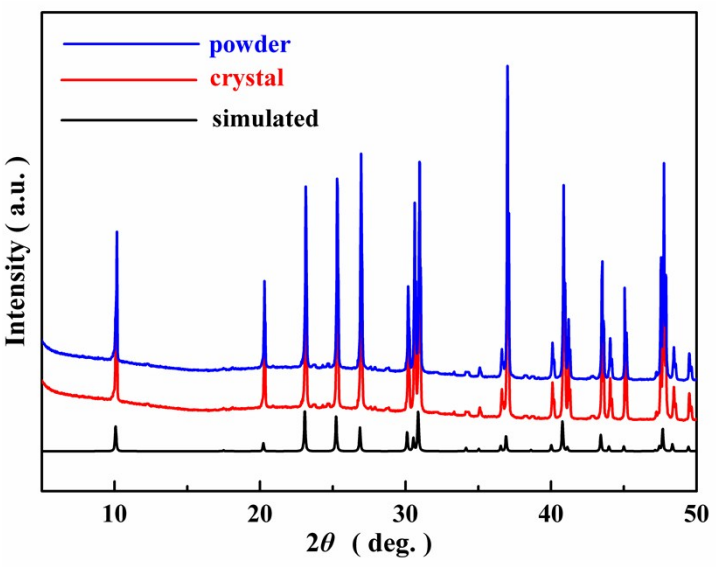

Figure S1. Simulated and measured powder X-ray diffraction patterns of $In[Ba_3Cl_3F_6]$.

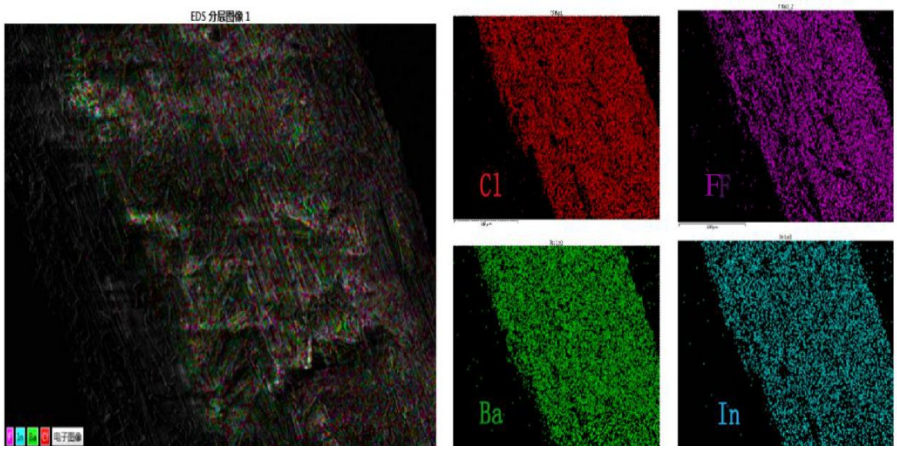

Figure S2. Scanning Electron Microscope (SEM) image of $In[Ba_3Cl_3F_6]$ and its elemental distribution maps.

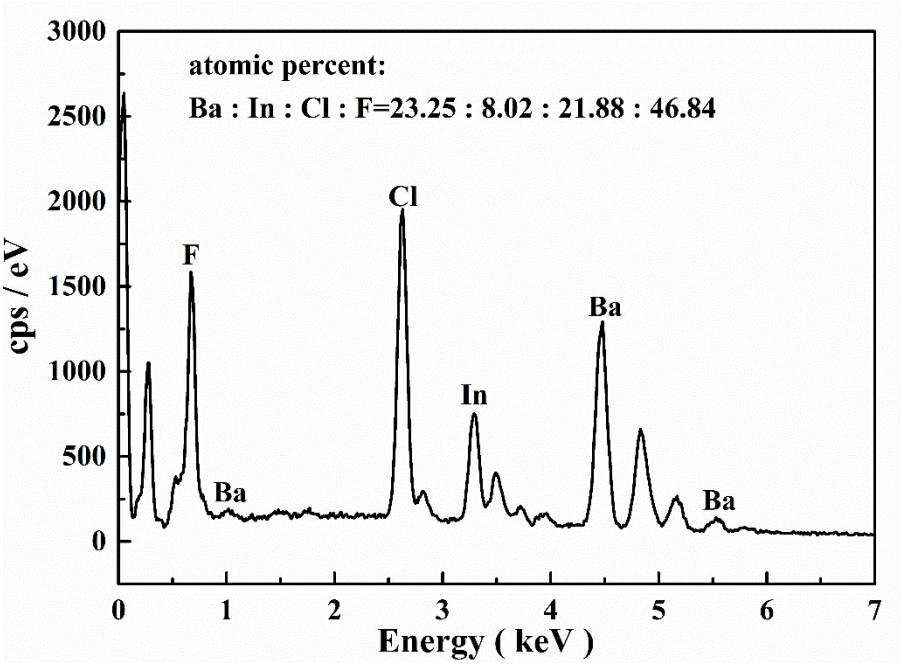

Figure S3. Energy Dispersive Spectrometer (EDS) of $In[Ba_3Cl_3F_6]$.

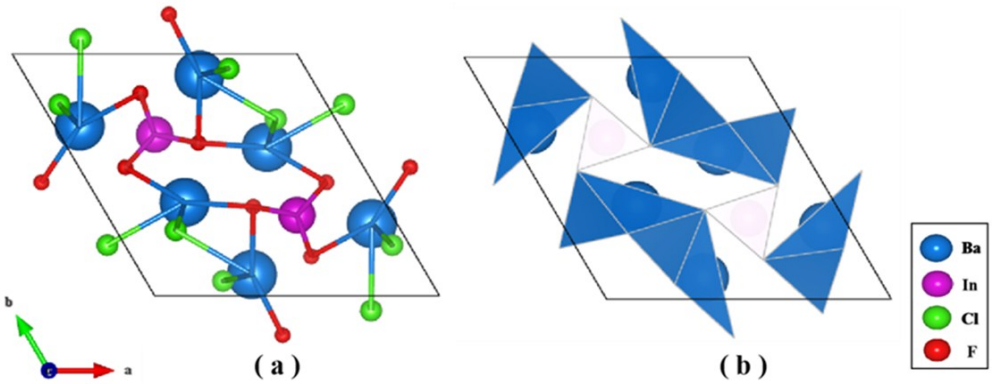

Figure S4. The structure of $In[Ba_3Cl_3F_6]$ viewed along the c-axis.

REFERENCES

1. P. Kubelka, F. Munk, Z. Tech, *Physical.,* 1931, **12**, 886-892.

2. S. Tandon, J. Gupta, *Phys. Status. Solidi.,* 1970, **38**, 363-367.

3. R. H. Blessing, *Acta. Crystallogr. A.*, 1995, **51**, 33-38.

4. G. M. Sheldrick, *Acta. Crystallogr. Sect. A.,* 1998.

5. D. Cruickshank, *Acta. Crystallogr.*, 1956, **9**, 747-753.